RESEARCH ARTICLE

**Editorial Process:** Submission:03/24/2024 Acceptance:08/11/2024

# Analyzing RPM and RGSC Infrared Camera Sensitivity: A Comparative Study of Breathing Cycle Replication Verifications and Limitations

**Arun Balakrishnan[1,2], Padmanabhan Ramesh Babu[2]***

## Abstract

**Objective:** This study addresses challenges in delivering high radiation doses and managing organ motion in Stereotactic Body Radiation Therapy (SBRT) for thoracic and abdominal cancer. It evaluates Varian's Real Time Position Management (RPM) system's infrared camera sensitivity during crucial Four-Dimensional computed tomography (4D-CT) scans for planning and treatment. The analysis includes CT simulator, LINAC (Novalis Tx and TrueBeam STx). This research enhances SBRT precision by offering insights into RPM and RGSC system performance across machines, impacting treatment planning and delivery optimization. **Methods:** The QUASAR™ Respiratory Motion Assembly phantom is aligned with precision using lasers. It is configured with either six-dot reflective or four-dot lens marker blocks featuring a retroreflective marker placed on the phantom's surface. Motion is induced by adjusting the amplitude, and the camera position is finely tuned to monitor the marker's movements. This investigation entails variations in seconds per breath (SPB) within the Quasar breath platform, specifically at intervals of 2.0, 2.5, 3.0, 3.5, 4.0, 4.5, and 5.0 seconds while maintaining a 1cm amplitude camera setting. **Result:** For TrueBeam-STx: Ensure SPB values are kept above 1.8 seconds for accurate replication. For Novalis-Tx: Stay within an SPB range of up to 2.0 seconds for reliable reproducibility. For CT Simulator: Optimal replication up to an SPB of 2.2 seconds; avoid SPB values below 1.8 seconds for reliable detection. **Conclusion:** Data for TrueBeam-STx, Novalis-Tx, and the CT simulator shows discrepancies in replicating the breathing cycle as Seconds Per Breath (SPB) decreases. Effective Infrared (IR) sensitivity is observed until SPB thresholds: 1.8s (TrueBeam-STx), 2.2s (Novalis-Tx), and 2.2s (CT simulator). We should consider values equal to or greater than the mentioned breathing periods. Variations in replicating breathing cycles signal challenges in planning and delivering treatments, especially with lower SPB values. These insights guide clinicians to adapt treatments based on machine-specific capabilities for accurate and reproducible outcomes.

**Keywords:** TrueBeam-STx, Novalis-Tx, and the CT simulator, RPM and RGSC

*Asian Pac J Cancer Prev,* **25 (8)**, 2861-2868

## Introduction

Stereotactic Body Radiation Therapy (SBRT) represents a highly targeted approach for administering concentrated doses of radiation to cancerous tumors, with the intent of minimizing damage to the surrounding healthy tissues. Initially stemming from intracranial Stereotactic Radiosurgery (SRS) in 1951, SBRT has evolved to become a versatile technique for treating tumors throughout the body [1-5].

One of the significant challenges in SBRT lies in achieving precision when targeting tumors, particularly when considering the impact of respiratory motion. The dynamic nature of respiratory motion introduces complexities during treatment, necessitating solutions to ensure accurate and effective radiation delivery. To address these challenges, the widespread adoption of four-dimensional CT (4D-CT) has emerged as a standard modality in SBRT [10]. Unlike traditional three-dimensional CT scans, 4D-CT accounts for the temporal dimension by capturing images at multiple phases of the respiratory cycle. This temporal information enables a more precise calculation of the margin required to accommodate tumor motion caused by breathing [6].

The adoption of 4D-CT in SBRT represents a crucial advancement in the field, enabling clinicians to address the challenges posed by respiratory motion with greater precision. This technology not only facilitates more accurate treatment planning but also contributes to the overall success and efficacy of SBRT in delivering targeted radiation therapy while minimizing the impact on healthy surrounding tissues [7]. The challenge of

*[1]Division of Medical Physics, Department of Radiation Oncology, Tata Medical Center, Kolkata, West Bengal, India. [2]Department of Physics, School of Advanced Sciences, Vellore Institute of Technology, Vellore, Tamil Nadu, India. *For Correspondence: prameshbabu@vit.ac.in*

breathing-induced motion artifacts affecting CT scan quality necessitates innovative solutions for radiation treatment planning [8, 9]. While deep inspiration breath-hold techniques are common in diagnostic scans, they prove impractical for CT Simulation in radiation treatment planning due to extended treatment durations. Overcoming this limitation involves generating CT image volumes covering the entire respiratory cycle, allowing observation of tumor movement under normal breathing conditions. The predominant method utilizes slow acquisition correlated with a respiratory signal, creating 4D-CT volumes [10-12].

In the context of SBRT, in this study introduces a free-breathing phase or respiratory amplitude-gated treatment approach employing the RPM camera. The accuracy of the RPM camera is validated using the QUASAR phantom, a versatile tool designed for quality assurance (QA) testing in radiation therapy systems.

The investigation assesses the RPM camera's sensitivity across three different machines: a 16-slice GE CT simulator with RPM camera version 1.7 MR2, Novalis Tx with a static RPM camera, and TrueBeam STx with RPM camera version 2.5. The evaluation involves RPM 3D reflector block marker and TrueBeam reflector block application in the RPM console system [13-18]. Also, the study compares and converts breathing pattern data from the RPM system to the Respiratory Gating for Scanners (RGSC) system.

Furthermore, sinusoidal breath pattern plots are analysed for both RPM and RGSC markers, considering various Seconds Per Breath (SPB) values. This comprehensive study provides insights into the RPM camera's sensitivity across diverse machines and compares breathing patterns under different SPB conditions. The findings contribute valuable information for quality assurance in radiation therapy systems, enhancing the understanding of respiratory motion management in the context of SBRT [19-26].

## Materials and Methods

*Phantom Design and Simulation*

The QUASAR phantom is a versatile QA tool for radiation therapy systems, conducting a wide range of tests including dosimetric and non-dosimetric evaluations. It features a multipurpose body phantom with CT imaging test objects and accommodates inserts for respiratory motion platforms. Tailored for End-to-End QA, it adapts to evolving technology with options for enhancement. The QUASAR Respiratory Motion Phantom is a programmable breathing simulator with software for downloading patient respiratory waveforms as depicted in Figure 1. Its dynamic motion offers a realistic representation for comprehensive QA testing in radiotherapy [2, 3].

*Infrared tracking camera*

The infrared tracking camera is equipped with a set of LEDs, emitting infrared light aligned with the camera's field of view, as depicted in Figure 2. A marker block, containing reflective dots, interacts with the emitted infrared light, and the camera captures the reflected signal. Subsequently, the software utilizes this signal to monitor and analyze the motion of the dots, corresponding to the dynamic movement of the chest or abdomen.

*Marker block*

The marker block, made of lightweight plastic, comes in two variants: a six-dot and a four-dot lens reflective marker. The six-dot variant has a domino shape with reflective markers on the front side facing the RPM camera assembly, while the four-dot lens marker has reflective markers angled for proper placement. The marker block remains consistently placed on the breathing simulation platform, ensuring continuous visibility to the tracking camera for 3D real-time monitoring of patient position. Standardization ensures precision, with the front IR reflector of the six-dot marker aligning with the center positioning marker of the four-dot lens marker, ensuring consistency throughout the study [17].

*Predictive Filter*

The patented Predictive Filter, an essential element of the RPM software, plays a crucial role in monitoring and predicting the breathing patterns. The initial step involves using the first four breathing patterns to construct a reference breathing pattern, calculating parameters such as the time of inspiration, expiration, and breathing period. The base value is set at the end of inspiration. Once the reference pattern is established, the Predictive Filter continually verifies whether successive breath patterns align with this reference.

*Reflector Marker*

Figure 3 illustrates the RPM console software windows, showcasing the six-dot reflector marker and the four-dot lens reflector marker. In the event of any deviation or interruption in the predicted breathing pattern caused by the cessation of phantom movement, the Predictive Filter promptly detects this discrepancy. Subsequently, the RPM system takes immediate action by gating off the radiation beam, ensuring both patient safety and treatment accuracy.

*Imaging for Treatment Planning*

Stable breathing is established before and during image acquisition with the aid of RPM.

*Prospective gated imaging*

During prospectively gated imaging, the CT scanner utilizes the RPM trigger signal to coordinate image acquisition with respiratory movements. Before initiating the scan, therapists define gating thresholds, and the scanner captures images precisely when the marker block aligns within the predetermined thresholds. This method produces a single-gated volumetric data set.

*Retrospective image acquisition*

In the case of retrospective image acquisition, the CT scanner continuously captures images, spanning at least one complete respiratory cycle at every couch position. Following the image acquisition phase, the CT image set is aligned with the RPM reference motion file. The images are organized into specific phase bins, each corresponding

to different stages in the respiratory cycle. Subsequently, an assessment is carried out to identify the most suitable phase for treatment. The chosen phase bin of images is then directed to the treatment planning stage.

*4D-CT Imaging in Computed Tomography Simulator Image Acquisition*

The GE Light Speed Xtra 16-slice CT-Simulator, coupled with the RPM system from Varian Medical Systems, was used to acquire a 4D-CT image set. The RPM system includes a six-dotted marker block, a couch-mounted camera system with an IR illuminator, and specialized gating software. The marker block has dots reflecting IR rays, positioned with specific spacing. The RPM system constantly monitors the phantom's breathing pattern using the IR reflector and camera. Image acquisition is triggered by the RPM gating signal, with each image labeled with a respiratory signal for treatment planning [1]. The 4D image sets are organized into phase-wise bins.

*QUASAR Phantom Setup for IR Camera Sensitivity*

The QUASAR PHANTOM undergoes precise alignment on the treatment couch, facilitated by laser guidance. Atop the phantom, both a four-dot or six-dot marker retroreflective marker block is carefully placed, and adjustments are made to the camera's position for accurate tracking of the marker's motion, replicating its movement [2, 3]. The phantom's motion is initiated by manipulating the longitudinal linear cedar insert, representing lung density, and connected to a power supply. This insert also includes a 3 cm diameter spherical tumor replica, simulating tumor density. The breath platform is configured with a variable breathing period timer, measured in seconds per breath (SPB). This standardized setup is maintained consistently throughout all measurements, including CT imaging and treatment machines like Novalis Tx and TrueBeam STx. This standardized approach guarantees consistency and accuracy in capturing and analyzing respiratory motion across various imaging and treatment scenarios, ultimately enhancing the effectiveness and safety of treatments delivered using machines like Novalis Tx and TrueBeam STx..

*Comparison of RPM system to RGSC system with sinusoidal breath pattern*

Sinusoidal breath pattern plots were generated for each SPB setting, and comparisons were conducted across different SPB values, including 2, 2.5, 3.0, 3.5 sec, 4.0 sec, 4.5 sec, and 5.0 sec, with time measured in samples per second.

An accuracy comparison was executed to evaluate the generation of breathing waveforms using the RPM six-dot reflective marker versus the four -dot lens marker in the RPM CT console. The objective was to scrutinize the precision and consistency of breathing waveforms produced by these markers within the CT console environment.

## Results

*IR Camera Timer Reader Sensitivity*

The examination of camera timer reader sensitivity in 4D-CT using the QUASAR phantom across different medical devices, including the CT scanner, Novalis Tx, and TrueBeam STx, holds significance for SBRT treatments. Multiple SPB, spanning from 5 seconds to 1.3 seconds, were configured in the timer motor of the Quasar phantom's motion platform, as outlined in Tables 1, 2, and 3. Executing a one-amplitude sine wave motion cam produced a sinusoidal breathing pattern in the Quasar phantom, tracked within the RPM system of the Table-mounted CT console, Wall-mounted Novalis Tx Treatment RPM system, and Ceiling-mounted TrueBeam RGSC system. The recorded times of inspiration, expiration, and overall breathing period were measured and juxtaposed with the preset timer values, elucidated in Tables 1, 2, and 3. Plotting the data from all three machines revealed disparities in replicating the breathing cycle as SPB decreased as shown in figures 4a, 4b, and 4c. For the CT RPM console system (Table 1), a decremental

Table 1. Represented as the Timer Reader Sensitivity of Couch Mounted CT Console RPM System

| Breathing Phantom set value per cycle in SECONDS PER BREATH (SPB) in Seconds | Measured INSPIRATION TIME (Sec) | Measured EXPIRATION TIME (Sec) | Measured Breath time (Sec) | % of variation |
|---|---|---|---|---|
| 5 | 2.5 | 2.5 | 5 | 0 |
| 4.5 | 2.3 | 2.2 | 4.5 | 0 |
| 4 | 2 | 2 | 4 | 0 |
| 3.5 | 1.7 | 1.8 | 3.5 | 0 |
| 3 | 1.5 | 1.5 | 3 | 0 |
| 2.5 | 1.3 | 1.2 | 2.5 | 0 |
| 2 | 1 | 1 | 2 | 0 |
| 1.8 | 1 | 1.1 | 2.1 | -16.66 |
| 1.6 | 1.3 | 1.5 | 2.8 | -75 |
| 1.5 | 1.2 | 2.1 | 3.3 | -120 |
| 1.4 | 1.6 | 2.1 | 3.7 | -164.28 |
| 1.3 | 1.7 | 1.9 | 3.6 | -176.92 |

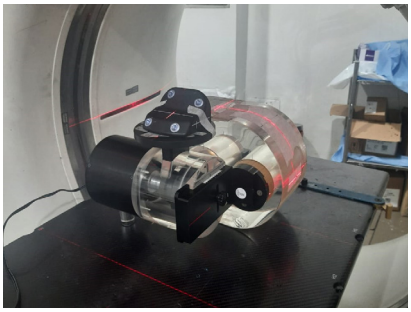

Figure 1. Shows that the Quasar Phantom™

Figure 2. Shows that the Infrared Tracking Camera

Table 2. Represented as the Timer Reader Sensitivity of Wall-Mounted Novalis Tx Console RPM System

| Breathing Phantom set value per cycle in SECONDS PER BREATH (SPB) in Seconds | Measured INSPIRATION TIME (Sec) | Measured EXPIRATION TIME (Sec) | Measured Breath time (Sec) | % of variation |
|---|---|---|---|---|
| 5 | 2.5 | 2.5 | 5 | 0 |
| 4.5 | 2.3 | 2.2 | 4.5 | 0 |
| 4 | 2 | 2 | 4 | 0 |
| 3.5 | 1.8 | 1.7 | 3.5 | 0 |
| 3 | 1.5 | 1.5 | 3 | 0 |
| 2.5 | 1.3 | 1.2 | 2.5 | 0 |
| 2 | 1 | 1 | 2 | 0 |
| 1.8 | 1 | 1 | 2 | -11.11 |
| 1.6 | 1.1 | 1.4 | 2.5 | -56.25 |
| 1.5 | 1.1 | 1.7 | 2.8 | -86.66 |
| 1.4 | 1.2 | 2.1 | 3.3 | -135.71 |
| 1.3 | 1.4 | 2.2 | 3.6 | -176.92 |

timer to a breathing period of 2.0 seconds exhibited good agreement. However, further reductions, even at 1.8 seconds, resulted in increased and erratic variations in the camera assembly's reader, accompanied by signal loss and a shift in the breathing period curve to red, impacting 4D-CT binning and gated treatments. The Wall-mounted Novalis Tx Treatment RPM system demonstrated similar outcomes (Table 2).

The discussion highlighted discernible distinctions in camera sensitivity resolution between the RPM Camera assembly and the RGSC system, with the latter displaying superior sensitivity. Specifically, the stereoscopic IR camera assembly in the RGSC system exhibited slightly higher sensitivity compared to the RPM Single camera assembly. In the IR camera of the RPM system, both in the CT console and the wall-mounted Novalis Tx, satisfactory agreement in timer reader sensitivity was observed for breathing periods of 2.0 seconds and above. However, in TrueBeam STx, the ceiling-mounted IR camera performed well only up to a breathing period

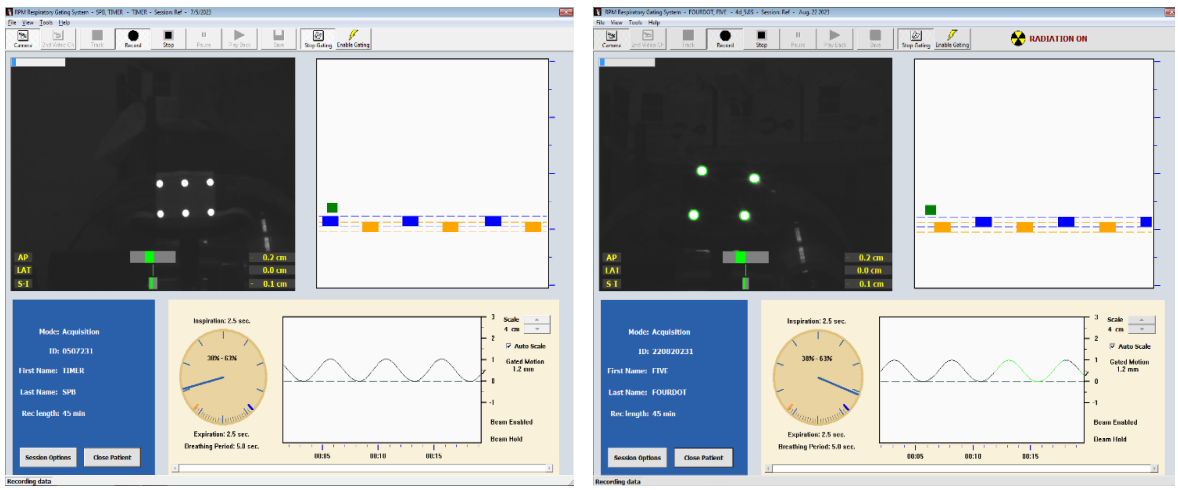


Figure 3. RPM Software Window of Six-Dot Reflective Marker and Four-Dot Lens Reflective Maker

Table 3. Represented as the Timer Reader Sensitivity of Ceiling-Mounted TrueBeam STx Console RGSC System

| Breathing Phantom set value per cycle in SECONDS PER BREATH (SPB) in Seconds | Measured INSPIRATION TIME (Sec) | Measured EXPIRATION TIME (Sec) | Measured Breath time (Sec) | % of variation |
|---|---|---|---|---|
| 5 | 2.5 | 2.5 | 5 | 0 |
| 4.5 | 2.3 | 2.2 | 4.5 | 0 |
| 4 | 2 | 2 | 4 | 0 |
| 3.5 | 1.8 | 1.7 | 3.5 | 0 |
| 3 | 1.5 | 1.5 | 3 | 0 |
| 2.5 | 1.2 | 1.3 | 2.5 | 0 |
| 2 | 1 | 1 | 2 | 0 |
| 1.8 | 0.9 | 0.9 | 1.8 | 0 |
| 1.6 | 0.8 | 0.8 | 1.6 | 0 |
| 1.5 | 0.8 | 0.9 | 1.7 | -13.33 |
| 1.4 | 0.7 | 1.2 | 1.9 | -35.71 |
| 1.3 | 0.7 | 2 | 2.7 | -107.69 |

of 1.8 seconds. Beyond this threshold, particularly at less than 2.0 seconds and 1.8 seconds of the breathing period, the IR camera's timer reader sensitivity response deteriorated. It registered random times for inhalation, expiration, and breathing period, leading to the loss of the breathing signal pattern when compared to the reference pattern of the RPM assembly system in the CT console, wall-mounted Novalis Tx, and ceiling-mounted IR camera assembly in TrueBeam STx. This observation emphasizes that for breathing periods less than 2.0 seconds, the IR camera's timer reader sensitivity is inadequate for effective breath-gating images.

From the Table 1 shows the time taken for inspiration and expiration for different set SPB value in Truebeam STx, which is used to plot a SPB versus breathing cycle graph and comparison. From the Table 2 shows time taken for inspiration and expiration for different set SPB values in Novalis Tx, which is used to plot a SPB versus breathing cycle graph and comparison. From the Table 3 Shows time taken for inspiration and expiration for different set SPB values in GE light speed CT machine, which is used to plot an SPB vs. breathing cycle graph and comparison.

The accuracy comparison of generating breathing waveforms using the RPM six-dot reflective marker versus the four-dot lens marker in the RPM CT console yielded positive results. Both reflective markers demonstrated good agreement, and all amplitudes were consistently recorded in negative values from the baseline in the RPM console's vxp file format.

However, it's essential to acknowledge a limitation observed in both the six-dot marker and the four-dot reflective marker. Specifically, when the breathing period was reduced to less than 2 seconds, the recording turned red, indicating a loss of signal for the breathing waveform. This implies that both markers encounter difficulties in maintaining signal integrity for breathing

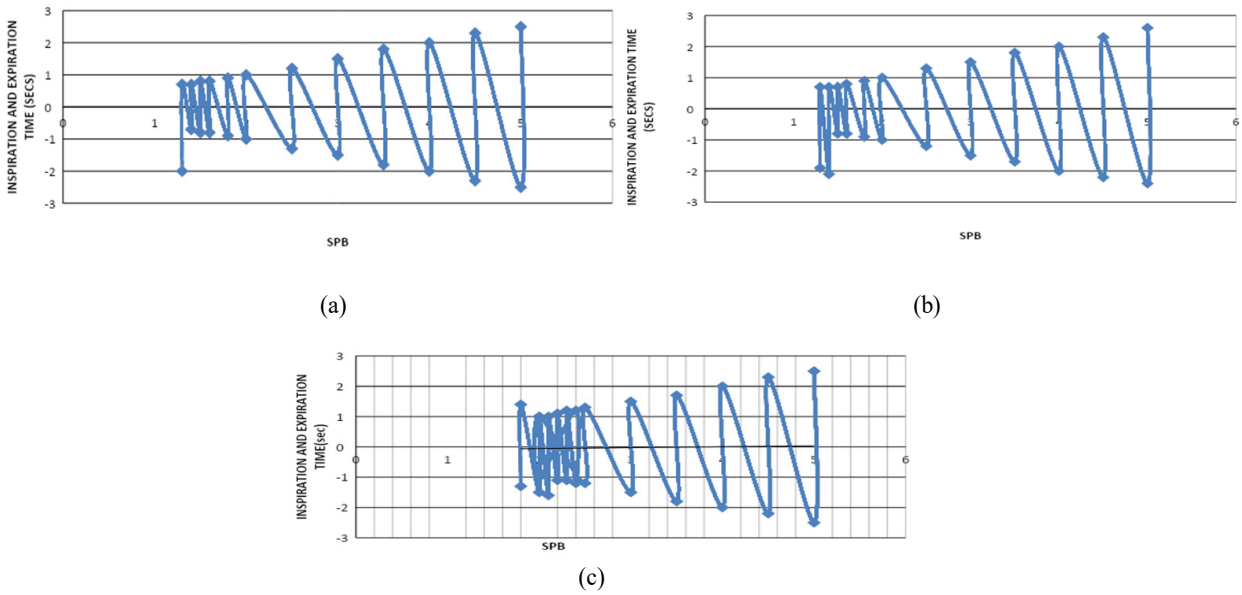


Figure 4. (a) SPB Vs. Breathing Cycle in Truebeam STx, (b) SPB Vs. Breathing Cycle in Novalis Tx, and (c) SPB Vs Breathing Cycle in GE- Lightspeed CT Simulator

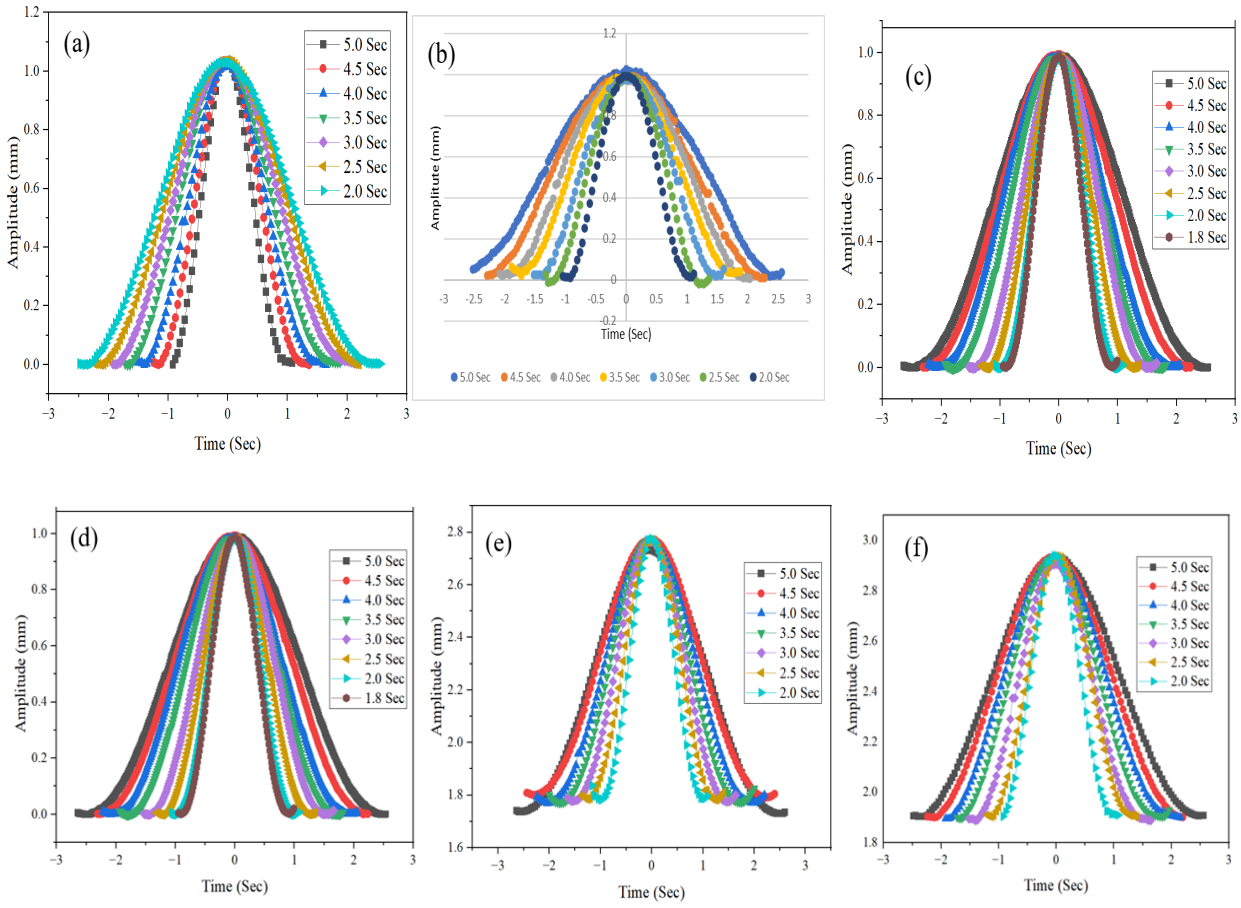


Figure 5 (a). Variable Breath Period of Ssingle Breath Pattern for Six-Dot Markers in CT, (b) Variable breath period of single breath pattern for six-dot markers in Novalis Tx, (c) Variable breath period of single breath pattern for four-dot markers in TrueBeam STx reference recorded pattern timer verification, (d) Variable breath period of single breath pattern for four-dot markers in TrueBeam STx during treatment timer verification, (e) Variable breath period of single breath pattern for four-dot lens markers in CT simulator and (f) Variable breath period of single breath pattern for six-dot markers in CT

periods shorter than 2 seconds. Notwithstanding this limitation, the comparison highlighted that both markers demonstrated good agreement across various breathing periods, consistently displaying amplitudes in the four-dot lens and six-dot RM reflective markers with the RPM camera assembly. This consistency is paramount for ensuring the reliable and accurate recording of breathing waveforms in the context of respiratory motion monitoring and management.

*Comparison of RPM System to RGSC system with sinusoidal breath pattern*

In the RGSC Treatment console of the True Beam machine, amplitude variations in all three directions (Left-Right, Anterior-Posterior, Head-Feet) are recorded at a significantly higher rate of 4000 66 samples per second (0.015 seconds per sample). This high sampling rate allows for detailed recording of amplitude and phase variations during respiratory motion, providing superior sensitivity compared to the RPM system.

Figures 4a to 4c visually depict the Anterior-Posterior amplitude depth variation over time, showcasing breathing waveforms generated from a sinusoidal motion breathing platform in the Quasar Phantom with six-dot markers. The RGSC system's higher sampling rate enables more accurate recording of amplitude and phase variations during respiratory motion compared to the RPM system.

The RPM console records Anterior-Posterior amplitude depth variation with time sample breathing waveforms executed from a sinusoidal motion breathing platform in the Quasar Phantom with six-dot markers at a considerably lower rate of 25 samples per second (2.4 0.04 seconds per sample).

Figures 5a to 5f demonstrate the advantages of four-dot lens reflectors over six-dot reflectors in camera sensitivity for RPM systems. These advantages include reducing interference and noise, improving the signal-to-noise ratio, enhancing tracking precision, and expediting data processing. These benefits collectively contribute to more reliable and accurate real-time position management in radiotherapy, ultimately enhancing patient safety and treatment efficacy.

## Discussion

The primary objective of the investigation was to evaluate the infrared (IR) camera sensitivity of the RPM system in the context of planning and treating thoracic

and abdominal cancer, particularly in Stereotactic Body Radiation Therapy (SBRT). The study focused on three different machines: TrueBeam STx, Novalis TX, and the CT Simulator. The plotted data revealed the ability of the IR camera to replicate the breathing cycle under different seconds per breath (SPB) values [10, 17 &18].

In TrueBeam STx, the breathing pattern was faithfully replicated up to an SPB of 1.4 seconds, with equal times for inspiration and expiration. However, deviations occurred for SPB values below 1.4 seconds, resulting in unequal times for inspiration and expiration. The IR camera in TrueBeam STx exhibited sensitivity up to an SPB of 1.4 seconds. Similar observations were made in Novalis TX, where the breathing cycle was effectively replicated until an SPB of 1.5 seconds. Beyond this threshold, the reproducibility was compromised, indicating that the IR camera sensitivity in Novalis TX extends up to 1.5 seconds.

Conversely, the IR camera in the CT Simulator room demonstrated the ability to replicate the respiratory cycle until an SPB of 2.2 seconds. However, beyond this threshold, disparities emerged in the times allocated for inspiration and expiration. Notably, at an SPB of 2.0 seconds, the IR camera lost its capability to track the six-dot marker, resulting in no signal captured by the RPM monitor. Consequently, the IR camera sensitivity in the CT Simulator was deemed effective up to an SPB of 2.2 seconds.

In summary, the study indicates that the IR camera sensitivity in the treatment machines (TrueBeam STx and Novalis TX) is comparable, with sensitivity extending up to an SPB value of 1.5 seconds. Conversely, the CT Simulator demonstrated sensitivity up to an SPB of 2.2 seconds. It is emphasized that the clinically utilized SPB value for 4D-CT scanning for SBRT patients in the institution typically falls within the range of 2.5-4 seconds.

The comparative analysis between the RPM system utilizing a six-dot marker and the TrueBeam Respiratory Gating System Console (RGSC system with a four-dot lens marker) reveals that the TrueBeam RGSC system boasts a higher sampling rate compared to the RPM system with a four-dot lens and six dot lens marker shown in figure 5e and 5f. Specifically, the six-dot marker in the RPM system registers approximately 80 times more in degrees of phase value and 160 times more in amplitude value across six dimensions. This notable enhancement in efficiency equips the RGSC system to effectively capture even subtle variations, especially those measured in sub-millimeters and with less than 2.5-degree phase values.

In conclusion, the study concludes that the RGSC system has successfully increased its efficiency to accommodate minor variations in breathing patterns. Additionally, it demonstrates the seamless conversion of breathing pattern waveforms from the RPM to the RGSC systems. The validation of phase values and amplitude values was carried out in the acquisition of breathing patterns, comparing Version 1.7 MR2 in the CT RPM system to the Static RPM camera-based treatment RPM console in Novalis TX and the Stereoscopic IR camera-based treatment console TrueBeam version 2.5. These findings underscore the improved performance and advanced capabilities of the TrueBeam RGSC system in accurately capturing respiratory motion patterns.

## Author Contribution Statement

Concept and data collection by Arun Balakrishnan, Guidance and supervision by P. Ramesh Babu; Manuscript evaluation and modification by Arun Balakrishnan and P. Ramesh Babu.

## Acknowledgements

Arun Balakrishnan is grateful for the support from Clinician colleagues, Senior Consultants Dr. Rimpa Achari, Dr. Sanjoy Chatterjee, Dr. Indranil Mallick, Dr. Santam Chakraborty, Dr. Moses Arun Singh, Dr. Tapesh Bhattacharjee and My Physics colleagues.

*Approval*

If it was approved by any scientific Body/ if it is part of an approved student thesis- Yes, Approved by Institution Review Board, Protocol Waiver NO: EC/WV/TMC/07/24.

*Ethical Declaration*

How the ethical issue was handled (name the ethical committee that approved the research)- This project involves publicly available datasets. This study is not involved with any patients or any healthy volunteers. Approved by Institution Review Board, Protocol Waiver NO: EC/WV/TMC/07/24.

*Data Availability: (if apply to your research)*

Data is available on request.

*Conflict of Interest*

Authors declare no conflict of Interest

## References

1. Ohara K, Okumura T, Akisada M, Inada T, Mori T, Yokota H, et al. Irradiation synchronized with respiration gate. International Journal of Radiation Oncology Biology Physics. 1989; 7(4):853-7. https://doi.org/10.1016/0360-3016(89)90078-3.
2. Balter JM, Ten Haken RK, Lawrence TS, Lam KL, Robertson JM. Uncertainties in CT-based radiation therapy treatment planning associated with patient breathing. International Journal of Radiation Oncology Biology Physics. 1996; 36(1):167-74. https://doi.org/10.1016/S0360-3016(96)00275-1.
3. Keall PJ, Starkschall G, Shukla HE, Forster KM, Ortiz V, Stevens CW, Vedam SS, et al. Acquiring 4D thoracic CT scans using a multislice helical method. Physics in Medicine & Biology. 2004; 49(10):2053. https://doi.org/10.1088/00319155/49/10/015.
4. Lanni TB, Jr., Grills IS, Kestin LL, Robertson JM. Stereotactic radiotherapy reduces treatment cost while improving overall survival and local control over standard fractionated radiation therapy for medically inoperable non-small-cell lung cancer. Am J Clin Oncol. 2011;34(5):494-8. https://doi.org/10.1097/COC.0b013e3181ec63ae.
5. Curran WJ, Jr., Paulus R, Langer CJ, Komaki R, Lee JS,

Hauser S, et al. Sequential vs. Concurrent chemoradiation for stage iii non-small cell lung cancer: Randomized phase iii trial rtog 9410. J Natl Cancer Inst. 2011;103(19):1452-60. https://doi.org/10.1093/jnci/djr325.
6. Borst GR, Sonke JJ, Betgen A, Remeijer P, van Herk M, Lebesque JV. Kilo-voltage cone-beam computed tomography setup measurements for lung cancer patients; first clinical results and comparison with electronic portal-imaging device. Int J Radiat Oncol Biol Phys. 2007;68(2):555-61. https://doi.org/10.1016/j.ijrobp.2007.01.014.
7. de Boer HC, van Sörnsen de Koste JR, Senan S, Visser AG, Heijmen BJ. Analysis and reduction of 3d systematic and random setup errors during the simulation and treatment of lung cancer patients with ct-based external beam radiotherapy dose planning. Int J Radiat Oncol Biol Phys. 2001;49(3):857-68. https://doi.org/10.1016/s0360-3016(00)01413-9.
8. Abbas G, Pennathur A, Landreneau RJ, Luketich JD. Radiofrequency and microwave ablation of lung tumors. J Surg Oncol. 2009;100(8):645-50. https://doi.org/10.1002/jso.21334.
9. Chang J, Mageras GS, Yorke E, De Arruda F, Sillanpaa J, Rosenzweig KE, et al. Observation of interfractional variations in lung tumor position using respiratory gated and ungated megavoltage cone-beam computed tomography. Int J Radiat Oncol Biol Phys. 2007;67(5):1548-58. https://doi.org/10.1016/j.ijrobp.2006.11.055.
10. Hugo GD, Yan D, Liang J. Population and patient-specific target margins for 4d adaptive radiotherapy to account for intra- and inter-fraction variation in lung tumour position. Phys Med Biol. 2007;52(1):257-74. https://doi.org/10.1088/0031-9155/52/1/017.
11. Sonke JJ, Lebesque J, van Herk M. Variability of four-dimensional computed tomography patient models. Int J Radiat Oncol Biol Phys. 2008;70(2):590-8. https://doi.org/10.1016/j.ijrobp.2007.08.067.
12. Seppenwoolde Y, Shirato H, Kitamura K, Shimizu S, van Herk M, Lebesque JV, et al. Precise and real-time measurement of 3d tumor motion in lung due to breathing and heartbeat, measured during radiotherapy. Int J Radiat Oncol Biol Phys. 2002;53(4):822-34. https://doi.org/10.1016/s0360-3016(02)02803-1.
13. Britton KR, Starkschall G, Tucker SL, Pan T, Nelson C, Chang JY, et al. Assessment of gross tumor volume regression and motion changes during radiotherapy for non-small-cell lung cancer as measured by four-dimensional computed tomography. Int J Radiat Oncol Biol Phys. 2007;68(4):1036-46. https://doi.org/10.1016/j.ijrobp.2007.01.021.
14. Donnelly ED, Parikh PJ, Lu W, Zhao T, Lechleiter K, Nystrom M, et al. Assessment of intrafraction mediastinal and hilar lymph node movement and comparison to lung tumor motion using four-dimensional ct. Int J Radiat Oncol Biol Phys. 2007;69(2):580-8. https://doi.org/10.1016/j.ijrobp.2007.05.083.
15. Gauthier JF, Varfalvy N, Tremblay D, Cyr MF, Archambault L. Characterization of lung tumors motion baseline using cone-beam computed tomography. Med Phys. 2012;39(11):7062-70. https://doi.org/10.1118/1.4762563.
16. Ecclestone G, Bissonnette JP, Heath E. Experimental validation of the van herk margin formula for lung radiation therapy. Med Phys. 2013;40(11):111721. https://doi.org/10.1118/1.4824927.
17. Hof H, Rhein B, Haering P, Kopp-Schneider A, Debus J, Herfarth K. 4d-ct-based target volume definition in stereotactic radiotherapy of lung tumours: Comparison with a conventional technique using individual margins. Radiother Oncol. 2009;93(3):419-23. https://doi.org/10.1016/j.radonc.2009.08.040.
18. Bradley JD, Nofal AN, El Naqa IM, Lu W, Liu J, Hubenschmidt J, et al. Comparison of helical, maximum intensity projection (mip), and averaged intensity (ai) 4d ct imaging for stereotactic body radiation therapy (sbrt) planning in lung cancer. Radiother Oncol. 2006;81(3):264-8. https://doi.org/10.1016/j.radonc.2006.10.009.
19. Ueda Y, Miyazaki M, Nishiyama K, Suzuki O, Tsujii K, Miyagi K. Craniocaudal safety margin calculation based on interfractional changes in tumor motion in lung sbrt assessed with an epid in cine mode. Int J Radiat Oncol Biol Phys. 2012;83(3):1064-9. https://doi.org/10.1016/j.ijrobp.2011.07.043.
20. Bissonnette JP, Franks KN, Purdie TG, Moseley DJ, Sonke JJ, Jaffray DA, et al. Quantifying interfraction and intrafraction tumor motion in lung stereotactic body radiotherapy using respiration-correlated cone beam computed tomography. Int J Radiat Oncol Biol Phys. 2009;75(3):688-95. https://doi.org/10.1016/j.ijrobp.2008.11.066.
21. Hugo GD, Liang J, Campbell J, Yan D. On-line target position localization in the presence of respiration: A comparison of two methods. Int J Radiat Oncol Biol Phys. 2007;69(5):1634-41. https://doi.org/10.1016/j.ijrobp.2007.08.023.
22. Grills IS, Hugo G, Kestin LL, Galerani AP, Chao KK, Wloch J, et al. Image-guided radiotherapy via daily online cone-beam ct substantially reduces margin requirements for stereotactic lung radiotherapy. Int J Radiat Oncol Biol Phys. 2008;70(4):1045-56. https://doi.org/10.1016/j.ijrobp.2007.07.2352.
23. Corradetti MN, Mitra N, Bonner Millar LP, Byun J, Wan F, Apisarnthanarax S, et al. A moving target: Image guidance for stereotactic body radiation therapy for early-stage non-small cell lung cancer. Pract Radiat Oncol. 2013;3(4):307-15. https://doi.org/10.1016/j.prro.2012.10.005.
24. Cai W, Dhou S, Cifter F, Myronakis M, Hurwitz MH, Williams CL, et al. 4d cone beam ct-based dose assessment for sbrt lung cancer treatment. Phys Med Biol. 2016;61(2):554-68. https://doi.org/10.1088/0031-9155/61/2/554.
25. Liu HW, Khan R, Nugent Z, Krobutschek K, Dunscombe P, Lau H. Factors influencing intrafractional target shifts in lung stereotactic body radiation therapy. Pract Radiat Oncol. 2014;4(1):e45-51. https://doi.org/10.1016/j.prro.2013.02.013.
26. Wang L, Feigenberg S, Fan J, Jin L, Turaka A, Chen L, et al. Target repositional accuracy and ptv margin verification using three-dimensional cone-beam computed tomography (cbct) in stereotactic body radiotherapy (sbrt) of lung cancers. J Appl Clin Med Phys. 2012;13(2):3708. https://doi.org/10.1120/jacmp.v13i2.3708.